ESAIM: M2AN 42 (2008) 175–192
DOI: 10.1051/m2an:2008002

ESAIM: Mathematical Modelling and Numerical Analysis
www.esaim-m2an.org

A C1-P2 FINITE ELEMENT WITHOUT NODAL BASIS

Shangyou Zhang[1]

Abstract. A new finite element, which is continuously differentiable, but only piecewise quadratic polynomials on a type of uniform triangulations, is introduced. We construct a local basis which does not involve nodal values nor derivatives. Different from the traditional finite elements, we have to construct a special, averaging operator which is stable and preserves quadratic polynomials. We show the optimal order of approximation of the finite element in interpolation, and in solving the biharmonic equation. Numerical results are provided confirming the analysis.

Mathematics Subject Classification. 65N30, 73C35.

Received December 11, 2006.

1. Introduction

The construction of C_1 finite elements is relatively difficult, especially when using low order piecewise polynomials. Most C_1 elements were constructed in Nineteen Seventies, or earlier, *cf*. [4,6], also [10,13,19,20,27,28]. Recently, we found a divergence-free, local basis for continuous P_1 elements on the criss-cross grids (Fig. 1(C)) in [22], which is originated in [1,21]. Because the C_0 divergence-free piecewise-P_1 vector space is the curl of C_1 piecewise-P_2 space on the same triangulation, in this paper we find the anti-derivatives of the above basis to get a local basis for the C_1-P_2 space on the criss-cross grid. Because the new local basis does not involve nodal-values of functions or their derivatives, we do not have a natural interpolation operator of the traditional finite elements. We have to construct a locally-averaging operator, preserving P_2 polynomials locally. It is shown that the newly-defined averaging interpolation operator is stable in various norms. Consequently, the new $C1$-$P2$ finite element space has the best order of approximation property, both in interpolation and in the Galerkin projection, when solving the biharmonic equations. The new averaging operator is similar to the average operators constructed by Clement [7] and by Scott and Zhang [25]. However, the polynomial preserving property is no longer trivial here. The techniques used in the paper could be applicable to some other cases.

We note that such a local $C1$-$P2$ basis is not known previously. However, the dimension of such $C1$-$P2$ space is known, studied by Morgan and Scott in [14], as a special case of the Strang's conjecture. Our construction of the new basis confirms the Strang's conjecture in some sense (see more discussion in Sect. 3). The method of representing a piecewise $C1$ polynomial basis without nodal function values or the derivatives appears previously in [17] too. We need to point out that there are two well-known C_1-P_2 elements, the Powell-Sabin element (Fig. 1(A)) and the Powell-Sabin-Heindl element (Fig. 1(B)), *cf*. [10,19,20]. It is obvious that the criss-cross type grid is more efficient in computation than the Powell-Sabin and Powell-Sabin-Heindl grids, considering

Keywords and phrases. Differentiable finite element, quadratic element, biharmonic equation, Strang's conjecture, criss-cross grid, averaging interpolation, non-derivative basis.

[1] Department of Mathematical Sciences, University of Delaware, DE 19716, USA. szhang@udel.edu

Article published by EDP Sciences

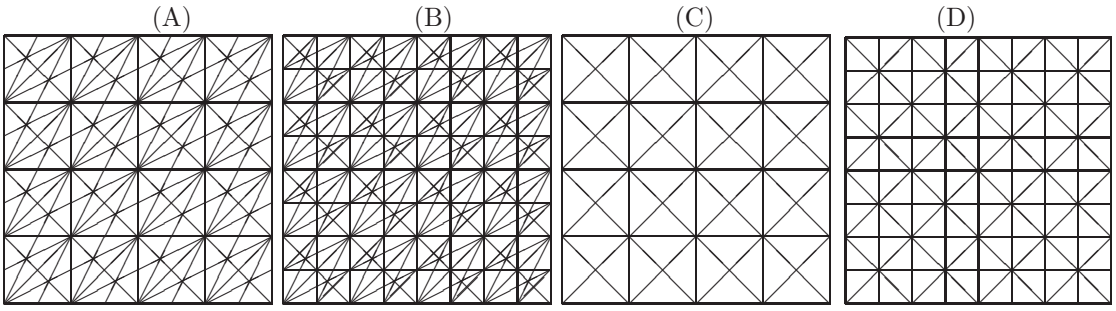

FIGURE 1. A PS grid, a PSH grid, a criss-cross Ω_h ($h = 1/4$) and a type-2 grid.

the number of triangles in an h-size region; *cf*. [11], for example. In addition, an advantage of a basis without nodal derivatives is its simplicity in implementation. Unlike the traditional C_1 conforming or nonconforming elements, such as Powell-Sabin elements or Morley elements ([19,20,29,30]), we do not need to do any scaling on the basis, and we have a better condition number for the discrete linear system too. We refer to Section 4 for more details. We need to point out that extensive studies have been done on a similar type of grids, the type-2 triangulation where the center of each square is connected to both four vertices and four mid-edge points (see Fig. 1(D)); *cf*. [12,15,26], and its counterpart in 3D, *cf*. [9,16,24].

The paper is divided into 4 sections. In Section 2, we define a local basis and finite element spaces for the new C_1-P_2 element on criss-cross grids. In Section 3, we introduce a locally-L_2-averaging operator, and establish the approximation properties of the C_1-P_2 element on the criss-cross grids. We then show the finite element space spanned by the local basis is complete, verifying the Strang's conjecture. In Section 4, we report some numerical results on the new element, and on the Powell-Sabin elements.

2. The C_1-P_2 element on criss-cross grids

The new C_1-P_2 element is defined on uniform grids, for example, shown as in Figure 1(C), *i.e.*, the domain can be subdivided into squares of a uniform size. For simplicity, we assume the domain is the unit square $\Omega = [0,1] \times [0,1]$.

We cut the domain into $(n \times n)$ squares, $Q_i = Q_{jk}$, and subdivide each small square into 4 triangles, $T_{i,l}$, by the two diagonal lines (shown in Fig. 2):

$$\begin{aligned}
\Omega &= \cup_{0\le j,k<n} Q_{jk},\\
Q_{jk} &= (x_j, x_{j+1}) \times (y_k, y_{k+1}),\ 0 \le j,\ k \le n-1,\\
Q_i &= T_{i,1} \cup T_{i,2} \cup T_{i,3} \cup T_{i,4},\quad \text{for}\quad i = jn + k + 1,\\
T_{i,1} &= \{(x,y) \mid 0 \le (y-y_k) \le h/2,\ (y-y_k) \le (x-x_j) \le h - (y-y_k)\},\\
T_{i,2} &= \{(x,y) \mid 0 \le (x-x_j) \le h/2,\ (x-x_j) \le (y-y_k) \le h - (x-x_j)\},\\
T_{i,3} &= \{(x,y) \mid (h/2) \le (x-x_j) \le h,\ h - (x-x_j) \le (y-y_k) \le (x-x_j)\},\\
T_{i,4} &= \{(x,y) \mid (h/2) \le (y-y_k) \le h,\ h - (y-y_k) \le (x-x_j) \le (y-y_k)\},\\
h &= 1/n.
\end{aligned} \tag{2.1}$$

Here $x_j = y_j = jh$. We call the triangulation Ω_h:

$$\Omega_h = \left\{ T_{i,m} \mid 1 \le m \le 4,\ 1 \le i \le n^2,\ n = \frac{1}{h} \right\}. \tag{2.2}$$

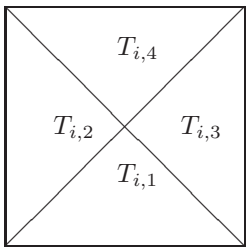

FIGURE 2. Each square Q_i is subdivided into four triangles.

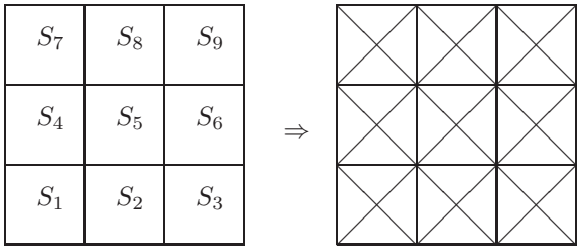

FIGURE 3. Each nodal basis function ϕ_i is supported on 9 squares (36 triangles).

On each (3×3) patch of squares, see Figure 3, we define one C_1-P_2 basis function ϕ_i. Here the index i is the index of the central square, *i.e.* $i = jn + k + 1$. ϕ_i is a C_1, but piecewise quadratic polynomial. We need to define ϕ_i on each of the 9 squares S_l, further on the 36 subtriangles, $T_{l,m}$, of S_l, see Figures 2–3. To describe ϕ_i, we map each of the 9 squares S_l to the referencing unit square $[0,1]^2 = \hat{Q}$ by affine mappings F_l, $1 \le l \le 9$. Then we let

$$\phi_i(x,y) = \begin{cases} \hat{\phi}_l(F_l^{-1}(x,y)) & \text{if } (x,y) \in S_l,\ 1 \le l \le 9, \\ \\ 0 & \text{elsewhere,} \end{cases}$$

where (see Fig. 3)

$$S_5 = Q_i = [x_a, x_a + h] \times [y_b, y_b + h], \quad i = an + b + 1.$$

Here $a = j - 1,\ j,\ j + 1,\ b = k - 1,\ k,\ k + 1$.

The definitions of basis functions $\hat{\phi}_l$ are listed below, and also depicted in Figure 4.

$$\hat{\phi}_1(\hat{x},\hat{y}) = \begin{cases} 0 & \text{on } \hat{T}_{1,1} \\ 0 & \text{on } \hat{T}_{1,2} \\ -\frac{1}{2} - \hat{x} - \hat{y} + \frac{\hat{x}^2}{2} + \frac{\hat{y}^2}{2} + \hat{x}\hat{y} & \text{on } \hat{T}_{1,3} \\ -\frac{1}{2} - \hat{x} - \hat{y} + \frac{\hat{x}^2}{2} + \frac{\hat{y}^2}{2} + \hat{x}\hat{y} & \text{on } \hat{T}_{1,4} \end{cases} \tag{2.3}$$

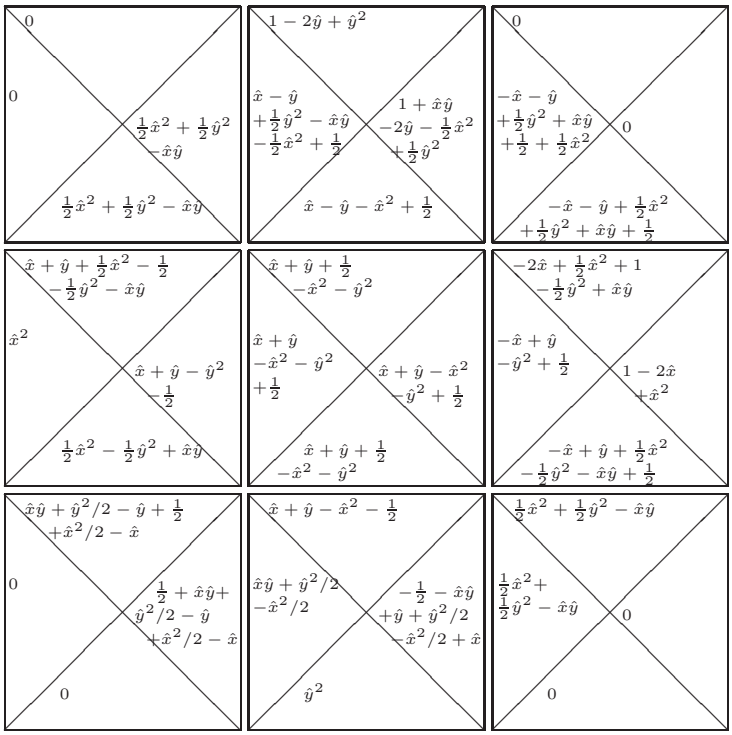

FIGURE 4. $\hat{\phi}_i$ on $[0,1]^2$, mapped from each of 9 squares.

$$\hat{\phi}_2(\hat{x},\hat{y}) = \begin{cases} \hat{y}^2 & \text{on } \hat{T}_{2,1} \\ -\frac{\hat{x}^2}{2} + \frac{\hat{y}^2}{2} + \hat{x}\hat{y} & \text{on } \hat{T}_{2,2} \\ -\frac{1}{2} + \hat{x} + \hat{y} - \frac{\hat{x}^2}{2} + \frac{\hat{y}^2}{2} - \hat{x}\hat{y} & \text{on } \hat{T}_{2,3} \\ -\frac{1}{2}\hat{x} + \hat{y} - \hat{x}^2 & \text{on } \hat{T}_{2,4} \end{cases} \tag{2.4}$$

$$\hat{\phi}_3(\hat{x},\hat{y}) = \begin{cases} 0 & \text{on } \hat{T}_{3,1} \\ \frac{\hat{x}^2}{2} + \frac{\hat{y}^2}{2} - \hat{x}\hat{y} & \text{on } \hat{T}_{3,2} \\ 0 & \text{on } \hat{T}_{3,3} \\ \frac{\hat{x}^2}{2} + \frac{\hat{y}^2}{2} - \hat{x}\hat{y} & \text{on } \hat{T}_{3,4} \end{cases} \tag{2.5}$$

$$\hat{\phi}_4(\hat{x},\hat{y}) = \begin{cases} \frac{\hat{x}^2}{2} - \frac{\hat{y}^2}{2} + \hat{x}\hat{y} & \text{on } \hat{T}_{4,1} \\ \hat{x}^2 & \text{on } \hat{T}_{4,2} \\ -\frac{1}{2} + \hat{x} + \hat{y} - \hat{y}^2 & \text{on } \hat{T}_{4,3} \\ -\frac{1}{2} + \hat{x} + \hat{y} + \frac{\hat{x}^2}{2} - \frac{\hat{y}^2}{2} - \hat{x}\hat{y} & \text{on } \hat{T}_{4,4} \end{cases} \tag{2.6}$$

$$\hat{\phi}_5(\hat{x},\hat{y}) = \begin{cases} \frac{1}{2}+\hat{x}+\hat{y}-\hat{x}^2-\hat{y}^2 & \text{on } \hat{T}_{5,1} \\ \frac{1}{2}+\hat{x}+\hat{y}-\hat{x}^2-\hat{y}^2 & \text{on } \hat{T}_{5,2} \\ \frac{1}{2}+\hat{x}+\hat{y}-\hat{x}^2-\hat{y}^2 & \text{on } \hat{T}_{5,3} \\ \frac{1}{2}+\hat{x}+\hat{y}-\hat{x}^2-\hat{y}^2 & \text{on } \hat{T}_{5,4} \end{cases} \tag{2.7}$$

$$\hat{\phi}_6(\hat{x},\hat{y}) = \begin{cases} \frac{1}{2}-\hat{x}+\hat{y}+\frac{\hat{x}^2}{2}-\frac{\hat{y}^2}{2}-\hat{x}\hat{y} & \text{on } \hat{T}_{6,1} \\ \frac{1}{2}-\hat{x}+\hat{y}-\hat{y}^2 & \text{on } \hat{T}_{6,2} \\ 1-2\hat{x}+\hat{x}^2 & \text{on } \hat{T}_{6,3} \\ 1-2\hat{x}+\frac{\hat{x}^2}{2}-\frac{\hat{y}^2}{2}+\hat{x}\hat{y} & \text{on } \hat{T}_{6,4} \end{cases} \tag{2.8}$$

$$\hat{\phi}_7(\hat{x},\hat{y}) = \begin{cases} \frac{\hat{x}^2}{2}+\frac{\hat{y}^2}{2}-\hat{x}\hat{y} & \text{on } \hat{T}_{7,1} \\ 0 & \text{on } \hat{T}_{7,2} \\ \frac{\hat{x}^2}{2}+\frac{\hat{y}^2}{2}-\hat{x}\hat{y} & \text{on } \hat{T}_{7,3} \\ 0 & \text{on } \hat{T}_{7,4} \end{cases} \tag{2.9}$$

$$\hat{\phi}_8(\hat{x},\hat{y}) = \begin{cases} \frac{1}{2}+\hat{x}-\hat{y}-\hat{x}^2 & \text{on } \hat{T}_{8,1} \\ \frac{1}{2}+\hat{x}-\hat{y}-\frac{\hat{x}^2}{2}+\frac{\hat{y}^2}{2}-\hat{x}\hat{y} & \text{on } \hat{T}_{8,2} \\ 1-2\hat{y}-\frac{\hat{x}^2}{2}+\frac{\hat{y}^2}{2}+\hat{x}\hat{y} & \text{on } \hat{T}_{8,3} \\ 1-2\hat{y}+\hat{y}^2 & \text{on } \hat{T}_{8,4} \end{cases} \tag{2.10}$$

$$\hat{\phi}_9(\hat{x},\hat{y}) = \begin{cases} \frac{1}{2}-\hat{x}-\hat{y}+\frac{\hat{x}^2}{2}+\frac{\hat{y}^2}{2}+\hat{x}\hat{y} & \text{on } \hat{T}_{9,1} \\ \frac{1}{2}-\hat{x}-\hat{y}+\frac{\hat{x}^2}{2}+\frac{\hat{y}^2}{2}+\hat{x}\hat{y} & \text{on } \hat{T}_{9,2} \\ 0 & \text{on } \hat{T}_{9,3} \\ 0 & \text{on } \hat{T}_{9,4}. \end{cases} \tag{2.11}$$

Here in (2.3)–(2.11) $\hat{T}_{l,m}$ is the image of the m-th subtriangle of S_l under the referencing mapping F_l. Finally, let $i = jn+k+1$ be the index of the square $Q_i = Q_{jk}$. Then we define a nodal basis ϕ_i, centered at the square $Q_{jk} = S_5$ and supported by the square and its 8 neighbor squares, by

$$\phi_i(x,y) = \begin{cases} \hat{\phi}_1(\frac{x-x_{j-1}}{h}, \frac{y-y_{k-1}}{h}) & \text{on } S_1 \\ \hat{\phi}_2(\frac{x-x_j}{h}, \frac{y-y_{k-1}}{h}) & \text{on } S_2 \\ \hat{\phi}_3(\frac{x-x_{j+1}}{h}, \frac{y-y_{k-1}}{h}) & \text{on } S_3 \\ \hat{\phi}_4(\frac{x-x_{j-1}}{h}, \frac{y-y_k}{h}) & \text{on } S_4 \\ \hat{\phi}_5(\frac{x-x_j}{h}, \frac{y-y_k}{h}) & \text{on } S_5 \\ \hat{\phi}_6(\frac{x-x_{j+1}}{h}, \frac{y-y_k}{h}) & \text{on } S_6 \\ \hat{\phi}_7(\frac{x-x_{j-1}}{h}, \frac{y-y_{k+1}}{h}) & \text{on } S_7 \\ \hat{\phi}_8(\frac{x-x_j}{h}, \frac{y-y_{k+1}}{h}) & \text{on } S_8 \\ \hat{\phi}_9(\frac{x-x_{j+1}}{h}, \frac{y-y_{k+1}}{h}) & \text{on } S_9. \end{cases} \tag{2.12}$$

The graph of $\phi_i(x,y)$ is shown in Figure 5.

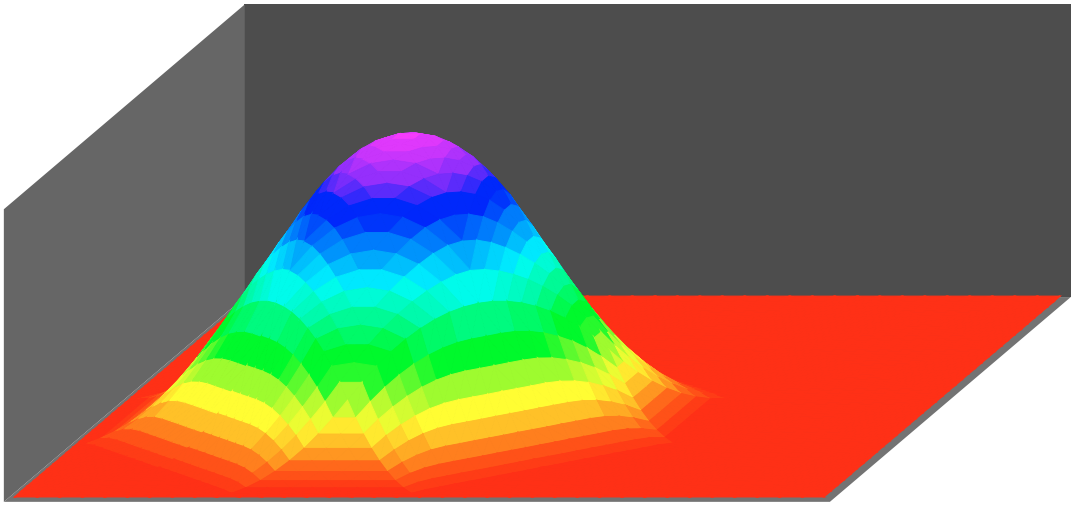

FIGURE 5. The 3D plot of a C_1-P_2 basis function, $z = \phi_i(x, y)$.

Before we define our finite element spaces, we need to show the basis functions are truly C_1, *i.e.*, continuously differentiable. It is done simply by checking two partial derivatives, $\mathrm{d}/\mathrm{d}x$ and $\mathrm{d}/\mathrm{d}y$. As a matter of factor, each vector $\mathbf{v}_i = \langle \frac{\mathrm{d}\phi_i}{\mathrm{d}y}, -\frac{\mathrm{d}\phi_i}{\mathrm{d}x} \rangle$ is zero-divergent. Such div-free vectors form a local basis for P_1-P_0 mixed-finite elements, approximating the velocity and the pressure in Stokes or Navier-Stokes equations, see [22]. This is in fact, how this new C_1-P_2 finite element was discovered.

Lemma 2.1. *The piecewise P_2 polynomial defined in (2.12) is a C_1 function.*

Proof. We need first check if ϕ_i is C_0. This is relatively easy. By letting $x = 0, 1, y, 1 - y$, and/or $y = 0, 1, x, 1 - x$ on two neighboring squares or triangles, in Figure 4, ϕ_i is shown to be continuous. This can also be seen from its graph in Figure 5.

Next, to show ϕ_i is C_1, we simply compute its two partial derivatives and check the derivatives. The two partial derivatives are shown in Figure 6. To check if the two derivatives (both are piecewise linear) are continuous, we only need to check their values at each vertex. This is done in Figure 7. □

We define the finite element spaces based on the local basis functions ϕ_i.

$$V_h = \mathrm{span}\left\{\phi_{jk}(x, y) \mid -1 \le j,\, k \le n,\, n = 1/h,\ (x, y) \in \Omega\right\}, \tag{2.13}$$

$$V_{h,0} = \mathrm{span}\left\{\phi_i = \phi_{jk} \mid 1 \le j,\, k < n - 2\right\}, \tag{2.14}$$

where in (2.14) we use both the index i and the double-index jk:

$$i = jn + k + 1.$$

We note that in (2.13) we introduced a ring of squares outside Ω. Then we could not use single index i there. For convenience, we denote the set of indices of $V_{h,0}$ by

$$J_h = \{i \mid i = jn + k + 1,\, 1 \le j,\, k < n - 2\}. \tag{2.15}$$

Since each basis function ϕ_i is C_1, we have then the following proposition that the linear combinations of such C_1 functions are also C_1.

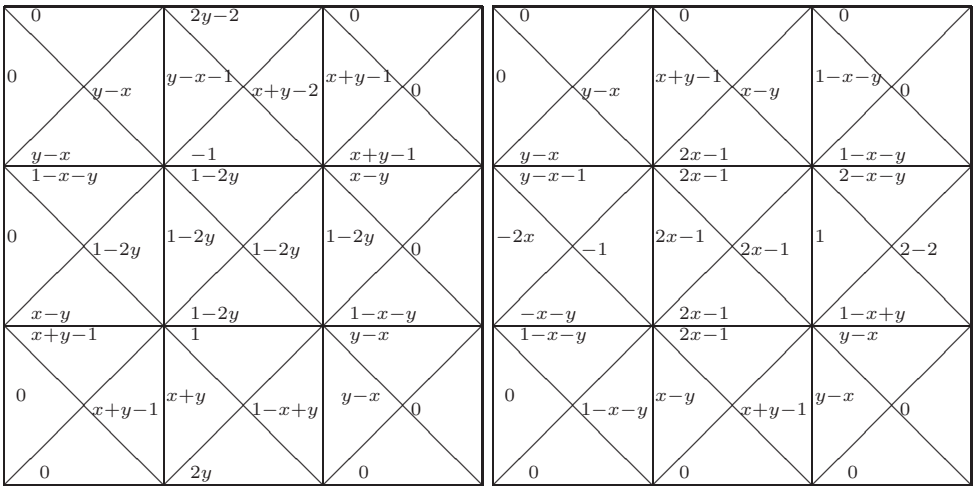

FIGURE 6. $\frac{\mathrm{d}\phi_i}{\mathrm{d}y}$ and $-\frac{\mathrm{d}\phi_i}{\mathrm{d}x}$, two C_0 piecewise P_1 polynomials.

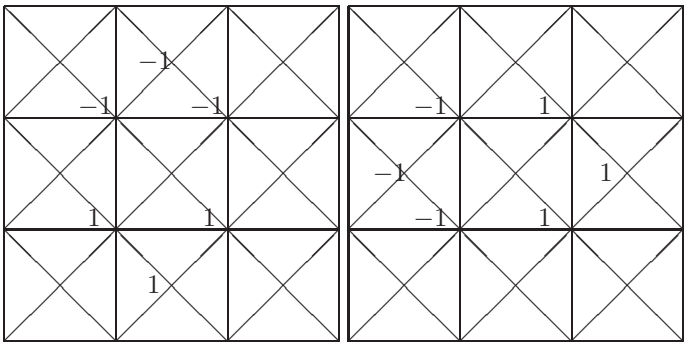

FIGURE 7. Nodal values of $\frac{\mathrm{d}\phi_i}{\mathrm{d}y}$ and $-\frac{\mathrm{d}\phi_i}{\mathrm{d}x}$ (a blank indicates a 0 value at the vertex).

Proposition 2.1. *The finite element spaces* (2.13)–(2.14) *are differentiable,* i.e.,

$$V_h \subset C_1, \quad V_{h,0} \subset C_1.$$

So we know now that the finite elements defined in (2.13)–(2.14) are C_1 functions and piecewise quadratic polynomials. What about the converse statement? It is also true shown in the following theorem.

Theorem 2.1. *Let $u \in C_1(\Omega)$ be a piecewise quadratic polynomial defined on Ω_h of* (2.2) *satisfying homogeneous boundary conditions*

$$u = 0 \quad \textit{and} \quad \frac{\partial u}{\partial n} = 0 \quad \textit{on } \partial\Omega.$$

Then

$$u \in V_{h,0}.$$

Proof. Let us consider the two partial derivatives of u, *i.e.*, $\operatorname{curl} u = \langle \partial u/\partial y, -\partial u/\partial x \rangle$. $\operatorname{curl} u$ is a C_0 piecewise linear polynomial vector function. Further it is divergence-free, *i.e.*, $\operatorname{div} \operatorname{curl} u \equiv 0$ on Ω. By Theorem 5.1 of [22], $\operatorname{curl} u$ is a linear combination of local div-free basis functions shown in Figure 6, *i.e.*,

$$\operatorname{curl} u = \sum_{i \in J_h} u_i \operatorname{curl} \phi_i.$$

Integrating both sides, by the homogeneous boundary conditions, we get (*cf.* [5,23])

$$u = \sum_{i \in J_h} u_i \phi_i \in V_{h,0}.$$

□

We note that Theorem 2.1 can be shown directly, without using the result [22], by the dimension counting of Strang's conjecture, which shall be discussed in next section.

3. Approximation property

From the definitions of basis functions ϕ_i and of finite element spaces V_h, it is not obvious that the discrete spaces do have the optimal order approximation property, *i.e.*, whether the spans of piecewise polynomials on 36 triangles do cover all global P_2 polynomials defined on the 36 triangles. We will show first that P_2 can be spanned by the basis functions ϕ_i. Then we will define an interpolation operator, based on a nodal L_2 orthogonal projection, and show its stability. With such an operator, it is then standard to establish the optimal order approximation property of the finite element space $V_{h,0}$.

Lemma 3.1. *Let $u(\hat{x}, \hat{y}) \in P_2([0,1]^2)$ be a quadratic polynomial. Then, u is a linear combination of $\{\hat{\phi}_i, 1 \le i \le 9\}$ defined in (2.3)–(2.11),* i.e., *there exist constants u_i such that*

$$u(\hat{x}, \hat{y}) = \sum_{i=1}^{9} u_i \hat{\phi}_i(\hat{x}, \hat{y}). \tag{3.1}$$

Proof. We can verify that,

$$\begin{cases} 1 = \hat{\phi}_1 + \hat{\phi}_3 + \hat{\phi}_5 + \hat{\phi}_7 + \hat{\phi}_9 \\ \hat{x} = \frac{3}{2}\hat{\phi}_1 - \frac{1}{2}\hat{\phi}_2 + \frac{1}{2}\hat{\phi}_3 + \hat{\phi}_5 - \hat{\phi}_6 + \frac{3}{2}\hat{\phi}_7 - \frac{1}{2}\hat{\phi}_8 + \frac{1}{2}\hat{\phi}_9 \\ \hat{y} = \hat{\phi}_1 + \frac{1}{2}\hat{\phi}_2 + \hat{\phi}_3 + \frac{1}{2}\hat{\phi}_5 - \frac{1}{2}\hat{\phi}_8 \\ \hat{x}^2 = 2\hat{\phi}_1 - \hat{\phi}_2 + \hat{\phi}_3 + \hat{\phi}_5 - \hat{\phi}_6 + 2\hat{\phi}_7 - \hat{\phi}_8 + \hat{\phi}_9 \\ \hat{y}^2 = \hat{\phi}_1 + \hat{\phi}_2 + \hat{\phi}_3 \\ \hat{x}\hat{y} = \frac{3}{2}\hat{\phi}_1 + \frac{1}{2}\hat{\phi}_5 - \frac{1}{2}\hat{\phi}_6 - \frac{1}{2}\hat{\phi}_8 + \frac{1}{2}\hat{\phi}_9. \end{cases} \tag{3.2}$$

As $u(\hat{x}, \hat{y})$ is a linear combination of $1, \hat{x}, \hat{y}, \hat{x}^2, \hat{y}^2$ and $\hat{x}\hat{y}$, by (3.2), $u(\hat{x}, \hat{y})$ is a linear combination of $\hat{\phi}_i(\hat{x}, \hat{y})$ on $[0,1]^2$. □

We remark that, to be more symmetric (see Fig. 3), we can rewrite two equations in (3.2) as

$$1-\hat{x}=\hat{\phi}_3-\frac{1}{2}\hat{\phi}_4+\frac{1}{2}\hat{\phi}_5+\frac{1}{2}\hat{\phi}_6+\hat{\phi}_9$$
$$(1-\hat{x})^2=\hat{\phi}_3+\hat{\phi}_6+\hat{\phi}_9.$$

Theorem 3.1. *Let $u(x,y)$ be a quadratic polynomial. Let $Q_i=Q_{jk}$ be any internal square of grid Ω_h,* i.e., *$i\in J_h$. Then, on Q_i, $u(x,y)$ is a linear combination of at most 9 basis function ϕ_l supported on the 9 squares surrounding Q_i.*

Proof. By Lemma 3.1, we have the following linear combination for the quadratic polynomial

$$u(x_j+\hat{x}h,y_k+\hat{y}h)=\sum_{l=1}^{9}u_l\hat{\phi}_l(\hat{x},\hat{y}).$$

Let $S_1=Q_{j-1,k-1},S_2=Q_{j,k-1}$, and so on as shown in Figure 3. We then have

$$u(x,y)=\sum_{l=1}^{9}u_l\phi_{S_l}(x,y)=\sum_{l=0,\pm1,\pm n,\pm n\pm1}p_l\phi_{l+i}(x,y)\quad\forall x\in S_5.$$ □

We define a local interpolation operator by considering L_2-inner products of functions in $V_{h,0}$ on each (3×3) patch of squares shown in Figure 3. Let M_i be such a macro-element patch centered at square $Q_i=S_5=Q_{jk}$, *i.e.*,

$$M_i=\cup_{l=1}^{9}S_l=Q_{j,k}\cup Q_{j\pm1,k}\cup Q_{j,k\pm1}\cup Q_{j\pm1,k\pm1}.$$

For simplicity, let $\{\phi_l\}$ denote the basis functions at the 9 squares S_l of M_i. This would be exactly the case $h=1/3$ if $M_i=\Omega$. We now let A be the matrix of L_2 inner products of the basis functions on M_i.

$$A=\left(\int_{M_i}\phi_l\phi_m\mathrm{d}x\,\mathrm{d}y\right)_{9\times9}.$$

Calculating by hand, or by any computer software, one would get

$$A=h^2\begin{bmatrix}
\frac{167}{180} & \frac{109}{240} & \frac{7}{288} & \frac{109}{240} & \frac{11}{60} & \frac{1}{240} & \frac{7}{288} & \frac{1}{240} & 0\\
\frac{109}{240} & \frac{751}{720} & \frac{109}{240} & \frac{11}{60} & \frac{59}{120} & \frac{11}{60} & \frac{1}{240} & \frac{1}{40} & \frac{1}{240}\\
\frac{7}{288} & \frac{109}{240} & \frac{167}{180} & \frac{1}{240} & \frac{11}{60} & \frac{109}{240} & 0 & \frac{1}{240} & \frac{7}{288}\\
\frac{109}{240} & \frac{11}{60} & \frac{1}{240} & \frac{751}{720} & \frac{59}{120} & \frac{1}{40} & \frac{109}{240} & \frac{11}{60} & \frac{1}{240}\\
\frac{11}{60} & \frac{59}{120} & \frac{11}{60} & \frac{59}{120} & \frac{7}{6} & \frac{59}{120} & \frac{11}{60} & \frac{59}{120} & \frac{11}{60}\\
\frac{1}{240} & \frac{11}{60} & \frac{109}{240} & \frac{1}{40} & \frac{59}{120} & \frac{751}{720} & \frac{1}{240} & \frac{11}{60} & \frac{109}{240}\\
\frac{7}{288} & \frac{1}{240} & 0 & \frac{109}{240} & \frac{11}{60} & \frac{1}{240} & \frac{167}{180} & \frac{109}{240} & \frac{7}{288}\\
\frac{1}{240} & \frac{1}{40} & \frac{1}{240} & \frac{11}{60} & \frac{59}{120} & \frac{11}{60} & \frac{109}{240} & \frac{751}{720} & \frac{109}{240}\\
0 & \frac{1}{240} & \frac{7}{288} & \frac{1}{240} & \frac{11}{60} & \frac{109}{240} & \frac{7}{288} & \frac{109}{240} & \frac{167}{180}
\end{bmatrix}.$$

From the inverse matrix of A, we can find the dual basis functions for the L_2 functional space of $\{\phi_{S_l}\}$. We are only interested in the dual of ϕ_{S_5}, denoted by ψ_i, *i.e.*,

$$\int_{M_i}\psi_i(x,y)\phi_{S_l}(x,y)\mathrm{d}x\,\mathrm{d}y=\begin{cases}1 & \text{if } l=5,\\ 0 & \text{if } l\neq5.\end{cases}$$

By the Riesz representation theorem, ψ_i is a linear combination of $\{\phi_{S_l}\}$ too. The coefficients for the linear combination is from the 5th column of matrix A^{-1}:

$$q = \frac{1}{553\,687h^2}\begin{pmatrix} 583\,704 \\ -970\,452 \\ 583\,704 \\ -970\,452 \\ 1\,743\,594 \\ -970\,452 \\ 583\,704 \\ -970\,452 \\ 583\,704 \end{pmatrix} = \frac{1}{h^2}\begin{pmatrix} 1.05421 \\ -1.75271 \\ 1.05421 \\ -1.75271 \\ 3.14906 \\ -1.75271 \\ 1.05421 \\ -1.75271 \\ 1.05421 \end{pmatrix}. \tag{3.3}$$

To be specific,

$$\psi_i = \sum_{l=1}^{9} q_l \phi_{S_l}, \tag{3.4}$$

where q_l is the lth component of vector q defined in (3.3). For convenience we extend $\psi_i(x, y)$ by 0 from M_i (9 squares) to the whole domain, and denote it by $\psi_i(x, y)$ too. The following lemma is implied simply by the definition of dual basis $\{\psi_i\}$.

Lemma 3.2. *Let ψ_i be defined in (3.4). For any $v = \sum_{i\in J_h} v_i\phi_i \in V_{h,0}$, it holds that*

$$\int_\Omega \psi_i v \,\mathrm{d}x\,\mathrm{d}y = v_i.$$

By $\{\psi_i\}$ we define an interpolation operator

$$\begin{aligned} I_h &: L_2(\Omega) \to V_{h,0}, \\ I_h &: v \mapsto v_h = I_h v = \sum_{i\in J_h} v_i\phi_i, \quad \text{where } v_i = \int_\Omega \psi_i v. \end{aligned} \tag{3.5}$$

Lemma 3.3. *The interpolation operator I_h defined in (3.5) is L_2 stable,* i.e.,

$$\|I_h v\|_{L_2(\Omega)} \le C\|v\|_{L_2(\Omega)} \quad \forall v \in L_2(\Omega),$$

where the constant C is independent of h.

Proof. We will estimate the following integral on two parts, on all the interior squares, and on a ring of squares along the boundary.

$$\begin{aligned} \|I_h v\|^2_{L_2(\Omega)} &= \int_\Omega \left(\sum_l v_l\phi_l\right)^2 \\ &= \int_{\cup_{Q_{jk}\cap\partial\Omega\neq\emptyset} Q_{jk}} \left(\sum_l v_l\phi_l\right)^2 + \int_{\cup_{i\in J_h} Q_i} \left(\sum_l v_l\phi_l\right)^2 \\ &= I_1 + I_2. \end{aligned}$$

Noting that each basis function is supported on 9 squares and has a maximal value 1 (see Fig. 4), we get

$$I_2 = \sum_{i\in J_h}\int_{Q_i}\left(\sum_l v_l\phi_l\right)^2 = \sum_{i\in J_h}\int_{Q_i}\left(\sum_{Q_l\subset M_i} v_l\phi_l\right)^2 \le \sum_{i\in J_h}\int_{Q_i} 9\sum_{Q_l\subset M_i} v_l^2\phi_l^2$$
$$\le \sum_{i\in J_h}\int_{Q_i} 9\sum_{Q_l\subset M_i} v_l^2 = 81h^2\sum_{i\in J_h} v_i^2.$$

By the definition of I_h in (3.5) and by the definition of ψ_i in (3.4), we get

$$v_i^2 = \left(\int_\Omega \psi_i v\right)^2 = \left(\int_{M_i}\psi_i v\right)^2 \le \left(\int_{M_i}\psi_i^2\right)\left(\int_{M_i} v^2\right)$$
$$\le \frac{q_5^2}{h^2}\left(\int_{M_i} 1\right)\left(\int_{M_i} v^2\right) < 4^2\cdot 9h^{-2}\int_{M_i} v^2.$$

Therefore

$$I_2 \le 81\cdot 4^2\cdot 9\sum_{i\in J_h}\int_{M_i} v^2 \le 81\cdot 4^2\cdot 9^2\int_\Omega v^2 = C\|v\|^2_{L_2(\Omega)}.$$

For the function $I_h v$ on the ring of squares along the boundary, due to the homogeneous boundary condition, the value is simply determined by the function value on the next ring of squares, *i.e.*, by the linear combinations of basis functions supported on the next ring of squares. Without loss of generality, we estimate the part of integral I_1 on the squares along the boundary $x = 0$ as follows:

$$\int_{\cup_{k=0}^{n-1}Q_{0k}}\left(\sum_l v_l\phi_l\right)^2 = \int_{\cup_{k=0}^{n-1}Q_{0k}}\left(\sum_{m=2}^{n-1} v_{n+m}\phi_{n+m}\right)^2 \le 3\cdot 3\sum_{m=2}^{n-1}\int_{Q_{1m}} v_{n+m}^2\phi_{n+m}^2.$$

The rest steps would repeat those in estimating I_2. The estimate of I_1 along the other three boundary edges is similar. So we have $I_1 \le C\|v\|^2_{L_2}$, and we proved the lemma. □

Lemma 3.4. *The interpolation operator I_h defined in (3.5) is H_1 stable,* i.e.,

$$\|I_h v\|_{H_1(\Omega)} \le C\|v\|_{H_1(\Omega)} \quad \forall v\in H_1(\Omega),$$

where the constant C is independent of h.

Proof. After Lemma 3.3, we need to show

$$|I_h v|_{H_1(\Omega)} \le C|v|_{H_1(\Omega)},\ \textit{i.e.},$$
$$\int_\Omega |\nabla I_h v|^2 \le C^2\int_\Omega |\nabla v|^2.$$

Then it is standard to insert piecewise constant functions approximating v:

$$\int_\Omega |\nabla I_h v|^2 = \sum_{j,k=0}^{n}\int_{Q_{j,k}}|\nabla I_h v|^2 = \sum_{j,k=0}^{n}\int_{Q_{j,k}}|\nabla\left(I_h v - \bar v_{jk}\right)|^2,$$

where we have chosen $\bar{v}_{jk}$ the average value of v on the square Q_{jk}, $\bar{v}_{jk} = \int_{Q_{jk}} v$. As each integral in the summation is on one small square $Q_{jk}(= S_5)$, $I_h v$ depends on the value of v on the 9 squares S_l shown in Figure 3, *i.e.*, $M_i(= M_{jk})$. Extending the constant function from Q_{jk} to M_i, we have

$$\int_\Omega |\nabla I_h v|^2 = \sum_{j,k=0}^{n} \int_{Q_{j,k}} |\nabla \left(I_h(v - \bar{v}_{jk})\right)|^2 = \sum_{j,k=0}^{n} \int_{Q_{j,k}} \left| \sum_{l=1}^{9} \tilde{v}_{S_l,jk} \nabla \phi_{S_i} \right|^2,$$

where $\tilde{v}_{S_l,jk}$ are the coefficients of $I_h(v - v_{jk})$ on M_{jk}. We note that as the piecewise constants are extended to 9 squares, these coefficients are no longer the same on different patches. Mapping each integral back to that on the reference square (the unit square), we would have $|\nabla \phi_{S_i}| \le Ch^{-1}$. Similar to the calculation in Lemma 3.3, we can derive

$$\begin{aligned} \int_\Omega |\nabla I_h v|^2 &\le C \sum_{i \in J_h} \sum_{l=1}^{9} \tilde{v}_{S_l,i}^2 \le Ch^{-2} \sum_{i \in J_h} \int_{M_i} (v - \bar{v}_i)^2 \\ &\le Ch^{-2} \sum_{i \in J_h} h^2 \int_{M_i} |\nabla v|^2 \le C |I_h v|^2_{H_1(\Omega).} \end{aligned}$$

□

Lemma 3.5. *The interpolation operator I_h defined in (3.5) is H_2 stable,* i.e.,

$$\|I_h v\|_{H_2(\Omega)} \le C \|v\|_{H_2(\Omega)} \quad \forall v \in H_2(\Omega),$$

where the constant C is independent of h.

Proof. The proof for Lemma 3.4 remains the same here, except the piecewise constants are replaced by piecewise linear functions, approximating v on each M_i patch. □

With the stability properties of I_h operator, it is standard ($cf.$ [4,25]) to show the approximation properties of I_h and the finite element spaces $V_{h,0}$. The trick is introducing the locally best approximation polynomials, as shown in the proof of Lemma 3.4, except using best quadratic polynomials instead of constants.

Theorem 3.2. *The finite element spaces $V_{h,0}$ defined in (2.14) have the optimal order of approximation,* i.e.,

$$\min_{v_h \in V_{h,0}} \left\{ \|v - v_h\|_{L_2} + h|v - v_h|_{H_1} + h^2 |v - v_h|_{H_2} \right\} \le Ch^3 \|v\|_{H_3} \quad \forall v \in H_{2,0}(\Omega) \cap H_3(\Omega).$$

We introduce next the biharmonic equation, its variational form and its finite element approximation. We then establish the best order convergence of the finite element solution. Let us consider the clamped plate bending problem, finding the solution of the following biharmonic equation with homogeneous boundary conditions,

$$\begin{cases} \Delta^2 u = f, & \text{in } \Omega = (0,1)^2, \\ u = 0 & \text{on } \partial\Omega, \\ \frac{\partial u}{\partial n} = 0 & \text{on } \partial\Omega. \end{cases} \tag{3.6}$$

Via integration by parts, we introduce the variational problem, finding $u \in H_{2,0}(\Omega)$ such that

$$\int_\Omega \Delta u \Delta v = \int_\Omega f v \qquad \forall v \in H_{2,0}(\Omega).$$

Let $V_{h,0}$ be defined in (2.14). The finite element solution u_h is defined by

$$a(u_h, v_h) = (f, v_h) \qquad \forall v \in V_{h,0}, \tag{3.7}$$

where $a(u,v) = \int \Delta u \Delta v$ and $(f,v) = \int fv$.

Theorem 3.3. *The finite element solutions from* (3.7) *converge at the optimal order,* i.e.,

$$|u - u_h|_{H_1} + h|u - u_h|_{H_2} \le Ch^2 \|f\|_{H_{-1}}.$$

Proof. The proof follows the Cea's lemma (*cf*. [4,6]) after the approximation property, Theorem 3.2. Then we apply the duality argument (*cf*. [4,6]) and the elliptic regularity of biharmonic equation on a convex polygonal domain (*cf*. [8]). □

As a side note, we will comment on a confirmation of the Strang's conjecture on the dimension of C_1 piecewise polynomials on triangles, by the new local basis functions ϕ_i. Let $S_p(\Omega_h)$ be the space of C_1 piecewise polynomials of degree p, on a general, simply connected, triangulation Ω_h. It is shown by Morgan and Scott [14] that

$$\dim S_p(\Omega_h) \ge \frac{(p+1)(p+2)}{2} T - (2p+1)E_0 + 3V_0 + \sigma, \tag{3.8}$$

where T is the number of triangles in Ω_h, E_0 the number of interior edges, V_0 the number of interior vertices, and σ the number of singular vertices in Ω_h. A vertex v is called singular if v is an interior vertex, if exactly four edges meet at v, and if the four edges form two straight lines. The Strang's conjecture is the equality in (3.8), under certain conditions (see [2,13,14] and references cited there). Nevertheless, the equality for (3.8) has been proved in [14] for C_1-P_2 elements on the criss-cross grid (Fig. 1(C)):

$$\begin{aligned} \dim S_2(\Omega_h) &= 6T - 5E_0 + 3V_0 + \sigma \\ &= 6(4n^2) - 5(2n(n-1) + 4n^2) + 3((n-1)^2 + n^2) + n^2 \\ &= n^2 + 4n + 3. \end{aligned} \tag{3.9}$$

By (2.13) the space V_h is spanned by $(n+2) \times (n+2) = n^2 + 4n + 4$ basis functions:

$$\{\phi_{j,k}, \quad -1 \le j,\ k \le n\}.$$

It is not surprising that the number of basis functions in V_h is one higher than the dimension of $S_2(\Omega_h)$. These $(n+2)^2$ basis functions $\{\phi_{jk}\}$ are linearly independent (on its supported domain $(-h, 1+h)^2$. But when restricted in the sub-domain $(0,1)^2$, they are not, because (see (3.2))

$$\begin{aligned} u_1(x,y) &= \sum_{j+k=\text{even}} \phi_{jk}(x,y) \equiv 1, \qquad 0 \le x,\ y \le 1, \\ u_2(x,y) &= \sum_{j+k=\text{odd}} \phi_{jk}(x,y) \equiv 1, \qquad 0 \le x,\ y \le 1. \end{aligned}$$

Therefore, we do have

$$\dim V_h = \dim S_2(\Omega_h).$$

We next consider the subspace $S_{2,0}$ of $S_2(\Omega_h)$, *i.e.*, the subspace in which the functions have homogeneous boundary conditions:

$$S_{2,0} = \left\{ u \in S_2(\Omega_h) \mid u|_{\partial\Omega} = 0, \quad \left.\frac{\partial u}{\partial n}\right|_{\partial\Omega} = 0 \right\}.$$

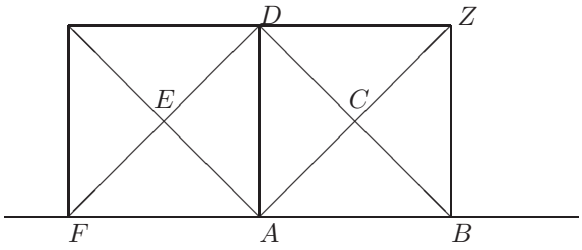

FIGURE 8. The restrictions on S_2 by the homogeneous boundary conditions.

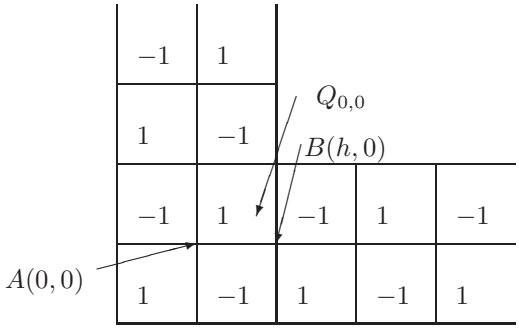

FIGURE 9. The restrictions on S_2 by the homogeneous boundary conditions.

From the analysis in Section 2, $S_{2,0} \subset V_h$. Let $u \in V_h$. Considering u on a boundary edge AB shown in Figures 8 and 9, because

$$\begin{aligned} u(A) = 0, \quad u\left(\frac{A+B}{2}\right) = 0, \quad u(B) = 0, \\ \frac{\partial u}{\partial n}(A) = 0, \quad \frac{\partial u}{\partial n}(B) = 0, \end{aligned} \tag{3.10}$$

we consider only 6 basis functions ϕ_{jk} (see (2.13)) which have a support over AB. There six basis functions are centered at the 6 boundary squares, either inside Ω or outside Ω, having A or B or both as a vertex or vertices. We can easily obtain the six coefficients of these six basis functions by solving a 5 by 6 homogeneous linear system of equations. For example, if AB is a corner edge as shown in Figure 9, then by conditions (3.10),

$$u|_{AB} = c\,(\phi_{-1,-1} - \phi_{0,-1} + \phi_{1,-1} - \phi_{-1,0} + \phi_{0,0} - \phi_{1,0})$$

for some constant c (might be zero). As (3.10) holds on all boundary edges, we conclude that all $u \in S_{2,0}$ form a one-dimensional vector space when restricted on $\partial\Omega$, *i.e.*, their coefficients are a common multiple of ± 1 shown in Figure 9. Now, because equations (3.10) hold on the two boundary edges of $Q_{0,0}$, u must be identical zero on the two subtriangles T_1 and T_2 of $Q_{0,0}$ at the corner $(0,0)$; see Figure 2. This leads to a conclusion that the coefficient of u for $\phi_{-1,-1}$ is zero. Therefore the coefficients of u for all boundary $\phi_{j,k}$ are zero. Therefore, $u \in V_{h,0}$. We conclude that the Strang's conjecture holds for $C1$-$P2$ spaces with homogeneous boundary conditions too, *i.e.*,

$$\dim(S_{2,0}) = \dim(V_{h,0}).$$

To show that the Strang's conjecture on the dimensions of $C1$ piecewise polynomials is quite complicated, we gave two naive ways of counting $\dim(S_{2,0})$. Let $u \in S_{2,0}$. Because u is a polynomial of degree two on a boundary

triangle ABC (see Fig. 8), $u|_{AB} = 0$ and $\frac{\partial u}{\partial n}\big|_{AB} = 0$, we have 5 restrictions posted on $u|_{\triangle ABC}$, listed in (3.10). So $u|_{\triangle ABC}$ is uniquely determined by the last degree of freedom, the value $u(C)$. We may conclude that we have 5 restrictions on each boundary edge for u, and that the total number of restrictions on u is

$$5E_b - 2V_b = 5(4n) - 2(4n) = 12n,$$

where E_b and V_b are number of boundary edges and vertices, respectively. Therefore we may claim incorrectly that $\dim S_{2,0} = \dim S_2 - 12n = n^2 - 8n + 3$. It is too low.

Let us try above arguments again (and incorrectly again). We have 5 restrictions on u due to the boundary conditions (3.10). u is determined by the "last degree of freedom", $u(C)$. Because of the C_1 continuity on edge AC (see Fig. 8), again we have five restrictions on $u|_{\triangle ACD}$. So, in turn, $u|_{\triangle ACD}$ is uniquely determined by the last freedom, the value $u(D)$. Repeating the same argument on $\triangle ADE$ and $\triangle AEF$, we conclude that there is "only one" restriction on u at the edge AF, *i.e.*, the nodal value

$$u(F) = 0.$$

Sequentially on the rest $4n - 3$ boundary vertices, we obtain the zero nodal value restriction only for $S_{2,0}$ functions. The total restrictions at the boundary is

$$R = 5 + 1 + (4n - 3) = 4n + 3.$$

Therefore, by (3.9), we get a too high number, $\dim S_{2,0}(\Omega) = n^2$.

Why do we post too many restrictions (3 per vertex) in the first try, but too few restrictions (1 per vertex) in the second try? This can be seen easily at a corner vertex. Let us assume B is a corner vertex of Ω. When we post 5 restrictions (3.10) on $u \in S_2$ at the edges AB and BZ (see Fig. 8), we can see the freedom $u(C)$ disappears, *i.e.*, $u(C) = 0$ because of the C_1 restriction on edge BC. Thus, the constraints on piecewise polynomials do depend on the configuration of triangulations.

4. Numerical tests

We will perform a simple numerical test on the newly proposed C_1 element. We will solve the biharmonic equation (3.6) on the unit square $(0, 1)^2$, where the exact solution is

$$u(x, y) = 2^8(x(1 - x)y(1 - y))^2,$$

then in (3.6) $f(x, y) = \Delta^2 u$. The exact solution is like the numerical solution, plotted in Figure 10.

We simply connecting the four corners of the square domain to get our first level triangulation; see the lower-central graph in Figure 11. Then we recursively refine each grid by subdividing each triangle into 4 subtriangles with 4 mid-edge points introduced. However, different from the traditional multigrid refinement shown on the left in Figure 11, we use the right refinement there, *i.e.*, connecting the midpoint of the longest edge to the opposite vertex. Under this new type of refinement, a criss-cross grid will be refined into another criss-cross grid (lower-right graph in Fig. 11). But the traditional multigrid refinement of a criss-cross grid would not generate a criss-cross grid (lower-left graph in Fig. 11).

In Table 1, we list the errors between the exact solution and the finite element solutions at several levels. The order of convergence of the finite element is consistent with that stated in Theorem 3.3.

Finally we make a numerical comparison between the new C_1-P_2 element and the Powell-Sabin element. The two elements are not quite comparable as the new C_1-P_2 element works on uniform grids only. But in this case, the new C_1-P_2 element is better both in coding simplicity and in computation efficiency. One Power-Sabin grid, used in our numerical test, is plotted in Figure 1(A), which is described as 4×4 grid in Table 2.

In Table 2, we can see that the number of triangles for the Powell-Sabin element is three times of that for the new C_1-P_2 element, in the $\#(\Omega_h)$ columns. The number of unknowns in the linear system for the Powell-Sabin

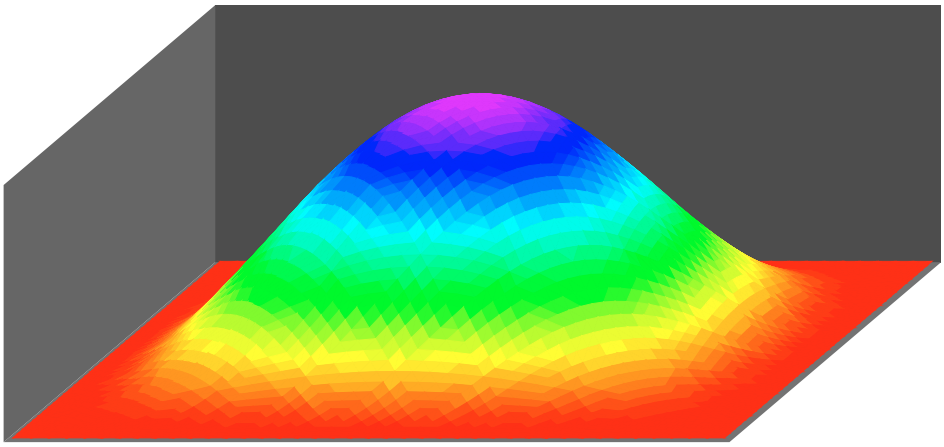

FIGURE 10. The 3D plot of C_1-P_2 finite element solution on level-4 grid.

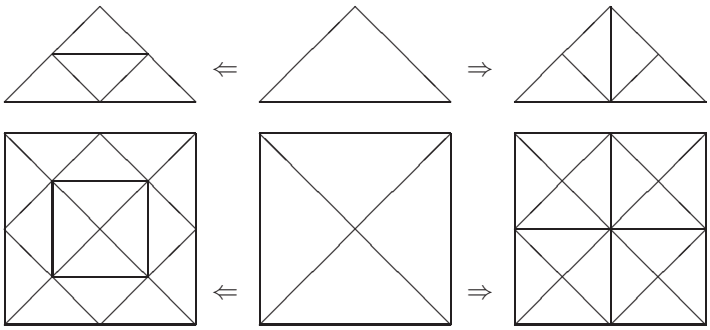

FIGURE 11. The standard multigrid refinement (left) and the longest-edge MG refinement.

TABLE 1. The convergence of C_1-P_2 element for the biharmonic equation.

Level	Grid	$\|u-u_h\|_{l_\infty}$	Order	$\|u-u_h\|_{H_2}$	Order
3	4×4	0.219555642	$--$	4.024573	$--$
4	8×8	0.058857283	1.8993	1.996800	1.01115
5	16×16	0.014900345	1.9819	0.990538	1.01141
6	32×32	0.003735972	1.9958	0.494153	1.00325
7	64×64	0.000934640	1.9990	0.246933	1.00084

element is $3(n-1)^2$, on a $(n\times n)$ grid, while that for the new C_1-P_2 element is only $(n-2)^2$. However, the H_2 error for the new element is slightly smaller. The nodal error $\|e_h\|_{l_\infty} = \|u-u_h\|_{l_\infty}$ is a little better for the Powell-Sabin element.

An advantage of the new basis for criss-cross grids is that it does not involve derivatives and it would produce a better condition number in general. In Table 2, we use n_i to denote the number of conjugate-gradient iterations. Without a diagonal scaling, *i.e.*, scaling the derivative nodal basis by h^{-1}, the iteration number n_1 is huge for Powell-Sabin elements. By the h^{-1}-scaling, the condition number of the Power-Sabin linear system would be reduced back to $O(h^{-4})$ and the number of iterations n_2 would be normal, though it is still more than 4 times bigger than that for the criss-cross grids (n_0) due to more unknowns. We would emphasize that the h^{-1}-scaling

TABLE 2. Comparison of new C_1-P_2 and Powell-Sabin elements.

	new C_1-P_2 element			the Powell-Sabin element					
Grid	$\#(\Omega_h)$	$\dim V_h$	n_0	$\#(\Omega_h)$	$\dim V_h$	n_1	n_2	$\|e_h\|_{l_\infty}$	$\|e_h\|_{H_2}$
2×2	16	0	0	48	3	2	2	0.6913	16.59
4×4	64	4	3	192	27	17	14	0.1525	8.45
8×8	256	36	8	768	147	169	82	0.0378	4.49
16×16	1024	196	32	3072	675	1155	370	0.0092	2.29
32×32	4096	900	139	12 288	2883	5275	1249	0.0023	1.15
64×64	16 384	3844	878	49 152	11 907	21 993	4776	0.0005	0.57

(and a h^{-2}-scaling for $\mathrm{d}^2v/\mathrm{d}x^2$-type basis functions) is necessary in the multigrid method in order to keep the constant rate of the iteration [32], *cf*. [3,18,31,33] for more information.

Acknowledgements. This work was done while the author visited the University of Science and Technology of China (USTC) during his sabbatical leave year, 2005–2006, and was presented in the International Conference on Partial Differential Equations and Numerical Analysis, held at Changsha, China, June 22–26, 2006. The author wishes to thank Chairman Falai Chen of the Department of Mathematics, USTC, and Professor Zhimin Zhang of Wayne State University, for their invitation and hospitality.

REFERENCES

[1] D.N. Arnold and J. Qin, Quadratic velocity/linear pressure Stokes elements, in *Advances in Computer Methods for Partial Differential Equations* **VII**, R. Vichnevetsky and R.S. Steplemen Eds. (1992).
[2] L.J. Billera, Homology of smooth splines: generic triangulations and a conjecture of Strang. *Trans. AMS* **310** (1988) 325–340.
[3] J.H. Bramble and X. Zhang, Multigrid methods for the biharmonic problem discretized by conforming C1 finite elements on nonnested meshes. *Numer. Functional Anal. Opt.* **16** (1995) 835–846.
[4] S.C. Brenner and L.R. Scott, *The Mathematical Theory of Finite Element Methods*. Springer-Verlag, New York (1994).
[5] F. Brezzi and M. Fortin, *Mixed and hybrid finite element methods*. Springer (1991).
[6] P.G. Ciarlet, *The Finite Element Method for Elliptic Problems*. North-Holland, Amsterdam (1978).
[7] P. Clément, Approximation by finite element functions using local regularization. *RAIRO Anal. Numér.* **R-2** (1975) 77–84.
[8] P. Grisvard, *Elliptic Problems in Nonsmooth Domains*. Pitman Pub. Inc. (1985).
[9] T. Hangelbroek, G. Nürnberger, C. Rössl, H.-P. Seidel and F. Zeilfelder, Dimension of C^1-splines on type-6 tetrahedral partitions. *J. Approx. Theory* **131** (2004) 157–184.
[10] G. Heindl, Interpolation and approximation by piecewise quadratic C1-functions of two variables, in *Multivariate Approximation Theory*, W. Schempp and K. Zeller Eds., Birkhäuser, Basel (1979) 146–161.
[11] M.-J. Lai, Scattered data interpolation and approximation using bivariate C1 piecewise cubic polynomials. *Comput. Aided Geom. Design* **13** (1996) 81–88.
[12] H. Liu, D. Hong and D.-Q. Cao, Bivariate C^1 cubic spline space over a nonuniform type-2 triangulation and its subspaces with boundary conditions. *Comput. Math. Appl.* **49** (2005) 1853–1865.
[13] J. Morgan and L.R. Scott, A nodal basis for C^1 piecewise polynomials of degree n. *Math. Comp.* **29** (1975) 736–740.
[14] J. Morgan and L.R. Scott, *The dimension of the space of C^1 piecewise-polynomials*. Research Report UH/MD 78, Dept. Math., Univ. Houston, USA (1990).
[15] G. Nürnberger and F. Zeilfelder, Developments in bivariate spline interpolation. *J. Comput. Appl. Math.* **121** (2000) 125–152.
[16] G. Nürnberger, C. Rössl, H.-P. Seidel and F. Zeilfelder, Quasi-interpolation by quadratic piecewise polynomials in three variables. *Comput. Aided Geom. Design* **22** (2005) 221–249.
[17] G. Nürnberger, V. Rayevskaya, L.L. Schumaker and F. Zeilfelder, Local Lagrange interpolation with bivariate splines of arbitrary smoothness. *Constr. Approx.* **23** (2006) 33–59.
[18] P. Oswald, Hierarchical conforming finite element methods for the biharmonic equation. *SIAM J. Numer. Anal.* **29** (1992) 1610–1625.
[19] M.J.D. Powell, Piecewise quadratic surface fitting for contour plotting, in *Software for Numerical Mathematics*, D.J. Evans Ed., Academic Press, New York (1976) 253–2271.
[20] M.J.D. Powell and M.A. Sabin, Piecewise quadratic approximations on triangles. *ACM Trans. on Math. Software* **3** (1977) 316–325.

[21] J. Qin *On the convergence of some low order mixed finite elements for incompressible fluids*. Ph.D. thesis, Pennsylvania State University, USA (1994).
[22] J. Qin and S. Zhang, Stability and approximability of the P1-P0 element for Stokes equations. *Int. J. Numer. Meth. Fluids* **54** (2007) 497–515.
[23] P.A. Raviart and V. Girault, *Finite element methods for Navier-Stokes equations*. Springer (1986).
[24] L.L. Schumaker and T. Sorokina, A trivariate box macroelement. *Constr. Approx.* **21** (2005) 413–431.
[25] L.R. Scott and S. Zhang, Finite element interpolation of nonsmooth functions satisfying boundary conditions. *Math. Comp.* **54** (1990) 483–493.
[26] T. Sorokina and F. Zeilfelder, Optimal quasi-interpolation by quadratic C^1-splines on type-2 triangulations, in *Approximation Theory* **XI**: *Gatlinburg 2004*, C.K. Chui, M. Neamtu and L.L. Schumaker Eds., Nashboro Press, Brentwood, TN (2004) 423–438.
[27] G. Strang, Piecewise polynomials and the finite element method. *Bull. AMS* **79** (1973) 1128–1137.
[28] G. Strang, The dimension of piecewise polynomials, and one-sided approximation, in *Conf. on Numerical Solution of Differential Equations, Lecture Notes in Mathematics* **363**, G.A. Watson Ed., Springer-Verlag, Berlin (1974) 144–152.
[29] M. Wang and J. Xu, Nonconforming tetrahedral finite elements for fourth order elliptic equations. *Math. Comp.* **76** (2007) 1–18.
[30] M. Wang and J. Xu, The Morley element for fourth order elliptic equations in any dimensions. *Numer. Math.* **103** (2006) 155–169.
[31] S. Zhang, An optimal order multigrid method for biharmonic C1 finite element equations. *Numer. Math.* **56** (1989) 613–624.
[32] X. Zhang, *Personal communication*. University of Maryland, USA (1990).
[33] X. Zhang, Multilevel Schwarz methods for the biharmonic Dirichlet problem. *SIAM J. Sci. Comput.* **15** (1994) 621–644.